3-10-2019

# Statistical algorithm for nonuniformity correction in focal-plane arrays

Majeed M. Hayat
*Marquette University*, majeed.hayat@marquette.edu

Sergio N. Torres
*University of Dayton*

Ernest Armstrong
*U.S. Air Force Research Laboratory*

Stephen C. Cain
*University of Dayton*

Brian Yasuda
*U.S. Air Force Research Laboratory*

Accepted version. *Applied Optics*, Vol. 38, No. 5 (March 10, 2019): 772-780. DOI. 

*Applied Optics*, Vol. 38, No. 5 (3/10/2019): 772-780. DOI. 

# Statistical algorithm for nonuniformity correction in focal-plane arrays

Majeed M. Hayat
University of Dayton
Sergio N. Torres
University of Dayton
Ernest Armstrong
U.S. Air Force Research Laboratory
Stephen C. Cain
University of Dayton
Brian Yasuda
U.S. Air Force Research Laboratory

## Abstract

A statistical algorithm has been developed to compensate for the fixed-pattern noise associated with spatial nonuniformity and temporal drift in the response of focal-plane array infrared imaging systems. The algorithm uses initial scene data to generate initial estimates of the gain, the offset, and the variance of the additive

electronic noise of each detector element. The algorithm then updates these parameters by use of subsequent frames and uses the updated parameters to restore the true image by use of a least-mean-square error finite-impulse-response filter. The algorithm is applied to infrared data, and the restored images compare favorably with those restored by use of a multiple-point calibration technique.

## 1. Introduction

The performance of focal-plane array (FPA) infrared imaging systems is known to be strongly affected by the spatial nonuniformity in the photoresponse of the detectors in the array. This nonuniformity results in a spatial pattern superimposed on the infrared image that reduces the resolving capability of the FPA imaging system.[1]-[3] What makes this problem even more challenging is that the spatial nonuniformity varies slowly in time.[4] For instance, external conditions, such as the surrounding temperature, variation in the transistor bias voltage, and the time-dependent nature of the object irradiance, can cause the gain and the offset of each detector to drift slowly and randomly in time. The task of any nonuniformity correction (NUC) algorithm is to compensate for the spatial nonuniformity and update the compensation as needed to account for the temporal variation in the detectors' responses.

Numerous NUC techniques have been reported in the literature. These techniques can be grouped into two main categories. The first category consists of NUC methods that rely on calibrating the FPA at distinct temperatures by use of flat-field data generated from a black-body radiation source.[1],[5],[6] Typically, calibration of the FPA often requires stopping the normal operation of the camera for the duration of the calibration. The second category consists of techniques that are scene based and require no calibration of the FPA. Scribner *et al*.[3],[7] developed a least-mean-square-based (LMS-based)-NUC technique that resembled adaptive temporal high-pass filtering. By adjusting the time constant of the filter, they used their algorithm to reduce the spatial noise caused by offset nonuniformity (the gain correction was performed separately). The effectiveness of their algorithm relies on the presence of motion in the image. A neural-network implementation of the adaptive LMS algorithm was also developed.[8] Narendra and Foss,[9] and more recently, Harris *et al*.,[10],[11] developed algorithms that continually compensate for the offset and the gain nonuniformity by using the concept of constant statistics, which postulates that the statistics (mean and variance) of the irradiance do not vary from detector to detector. The algorithm reported by Harris *et al*.[11] subtracts the estimated detector offset (estimated by a moving windowed time average of the detector voltage) and then normalizes the outcome by the detector gain (measured by a windowed $L_1$ norm of the voltage). Their method is motivated by clues from neurobiological (linear and nonlinear) adaptation. Using simulated data, they showed that their method compares well with the results obtained with Scribner's LMS algorithm.[7]

Cain *et al*.[12] considered a Bayesian approach to NUC and developed a maximum-likelihood algorithm that jointly estimates the high-resolution image, the detectors' parameters, and any possible spatial shift (arising from motion or vibration). The algorithm relies on the assumption that the image has Poissonian statistics and that the detector response is nonlinear. The performance of the maximum-likelihood algorithm[12] was shown to be comparable, in certain cases, to the performance of two-point calibration NUC. The algorithm is computationally extensive, and it is intended for cases in which only a few frames of data are available.

In this paper we develop a statistical algorithm that adaptively performs NUC, using the scene data. The correction is performed by a finite-impulse-response (FIR) LMS filter (i.e., a discrete-time Wiener filter) that involves current estimates of the gain, the offset, and the variance of the additive electronic noise. The model assumes a linear detector response and irradiance at each detector that is a uniformly distributed random variable. The gain, the offset, and the variance of the additive noise are all assumed to be time varying but approximately constant within certain blocks of time. As a new block of scenes is captured, the Wiener filter adapts itself to it by statistical extraction of the changes in the detector parameters and electronic noise. We applied the algorithm to data acquired by using an Amber FPA camera and were able to achieve NUC results that compare favorably with those obtained by using a multiple-point calibration method.

## 2. Model

In many applications sensors are operated in a range of irradiance within which detectors exhibit linear input–output characteristics. In this paper we adopt the following statistical linear model for the detector response. For the (*i*, *j*)th detector in the array, and at time *n*, the measured signal (detector response) $Y_{ij}(n)$ is given by the approximate linear relation

$$(1)\ Y_{ij}(n) = A_{ij}(n)X_{ij}(n) + B_{ij}(n) + N_{ij}(n),$$

where $A_{ij}(n)$ is the gain associated with (*i*, *j*)th detector at time *n*, $B_{ij}(n)$ is an offset voltage term, and $X_{ij}(n)$ is the irradiance collected by the detector during the integration time. For ease of notation the subscript *ij* is dropped from all the quantities with the understanding that all operations are performed on a pixel-by-pixel basis. The term $N(n)$ represents additive electronic noise that is modeled by a zero-mean Gaussian random variable that is statistically independent of the noise in other detectors. For simplicity it is assumed that the noise $N(n)$ is independent of the irradiance $X(n)$; however, information from black-body-radiation data shows a weak correlation between the noise variance and the irradiance.

The dependence of the gain and the offset on *n* is used to capture the temporal variation (or drift) in the parameters of the detector response. The gain and the offset are assumed to be statistically independent of the irradiance and the noise. We assume that, for each *n*, the collected irradiance $X(n)$ is a uniformly distributed random variable in some range $[x_{\min}, x_{\max}]$ constituting the range (common to all detectors) of possible irradiance levels prior to saturation. This assumption merely states that no *a priori* information on the scene is available other than the fact that it is in a certain range. It is also assumed that the temporal correlation in the irradiance is known {i.e., the autocorrelation function $E[X(l)X(m)]$ is assumed to be known}. In the examples considered in this paper, we obtained good correction by simply assuming that $X(l)$ and $X(m)$ are uncorrelated for $l \neq m$. The algorithm operates on an individual detector independently of all other detectors. Knowledge of the spatial statistics of the irradiance is therefore not required.

## 3. Description of the Algorithm

We first give a brief description of the algorithm. Suppose that an initial set of data corresponding to *n* in the range $-n_p \leq n \leq -1$ is used to generate estimates of the model parameters at time $n = 0$, i.e., for a given detector estimates of $A(0)$, $B(0)$, and $\sigma_{N,0}^2$ are available. These parameters are assumed to be

almost constant within the block of frames $0 \le n \le n_b$ and are denoted by $A_0$, $B_0$, and $\sigma_{N,0}^2$, respectively. The choice of the block length $n_b$ depends on how frequently adjustments to the estimated model parameters are required, which in turn depends on the type of the FPA and prior knowledge of the level of drift of the parameters. On the other hand, the required number of frames in the initial data, $n_p$, must be large enough to yield statistical stability and yet allow fast processing. Specific choices of $n_p$ and $n_b$ are given in Section 4.

The initial parameters $A_0$, $B_0$, and $\sigma_{N,0}^2$ can then be used in the design of a linear LMS estimate of $X(n)$, denoted by $\hat{X}(n)$, in the block of frames $0 \le n \le n_b$. The output of the linear LMS estimator $\hat{X}(n)$ is a weighted sum of the current scene $Y(n)$ and the past $L - 1$ frames, where $L \ge 1$ is a fixed parameter and is chosen on the basis of the knowledge of the temporal correlation of the irradiance.

For the next block of frames, $n_b < n < 2n_b$, the updated parameters $A_1$, $B_1$, and $\sigma_{N,1}^2$ must be computed by use of the gain and the offset from the previous block *and* from the scene data from the tail of the previous block in the range $n_b - n_p \le n \le n_b - 1$. A new LMS filter is then designed to generate $\hat{X}(n)$ in the block of frames indexed by $n_b \le n < 2n_b$, and so on.

There are therefore two interrelated operations involved in the algorithm: the periodic updating of the model parameters and the frame-by-frame estimation (restoration) of the signal. A block diagram of the algorithm is shown in Fig. 1. We now give a more detailed description of the algorithm.

## A. Initial Parameter Estimation

An initial estimate of the parameters $A_0$, $B_0$, and $\sigma_{N,0}^2$ must be obtained from a rich set of data. Rich data consist of a sequence of frames for which the signal $X$, in each detector, varies in the range $[x_{min}, x_{max}]$ common to all other detectors in the array. One way to generate such rich data is to expose the camera to a scene containing warm and cold objects and then move the camera in such a way that all detectors are eventually exposed to the same high and low levels of irradiance. Let

$$Y_{max}^{(0)} \triangleq \max_{-n_p \le n \le -1} \{Y(n)\}, Y_{min}^{(0)} \triangleq \min_{-n_p \le n \le -1} \{Y(n)\}.$$

By equating the values of $Y(0)$max and the $Y(0)$min to the maximum and the minimum, respectively, of Eq. (1) and ignoring the noise term, we obtain

$$(2)\ Y_{max}^{(0)} \approx A_0 \max_{-n_p \le n \le -1} \{X(n)\} + B_0,$$

$$(3)\ Y_{min}^{(0)} \approx A_0 \min_{-n_p \le n \le -1} \{X(n)\} + B_0.$$

By assuming that the range of temperatures used to generate the initial data is sufficiently large {i.e., comparable to $[x_{min}, x_{max}]$} and that all detectors are eventually exposed to the same range of irradiance, we obtain

$$\max_{-n_p \le n \le -1} \{X(n)\} \approx x_{max}, \min_{-n_p \le n \le -1} \{X(n)\} \approx x_{min},$$

for all detectors. The parameters $A_0$ and $B_0$ are then readily computed from expressions (2) and (3) as

$$(4)\ A_0 = \frac{Y_{max}^{(0)} - Y_{min}^{(0)}}{x_{max} - x_{min}},$$

$$(5)\ B_0 = Y_{max}^{(0)} - A_0 x_{max}.$$

To obtain an estimate of $\sigma_{N,0}^2$, we consider the one-step difference signal $D(n) \triangleq Y(n) - Y(n-1)$. Because the temporal variation in the irradiance is typically much slower than the variation in noise, we obtain

$$D(n) \approx N(n) - N(n-1).$$

Hence $\sigma_{N,0}^2$ can be estimated as one half of the sample variance of the difference signal $D(n)$:

$$(6)\ \sigma_{N,0}^2 = \frac{1}{2}\frac{1}{n_p}\sum_{n=-n_p}^{-1}\left[D(n) - \hat{D}(0)\right]^2,$$

where $\hat{D}(0)$ is the sample mean of the difference signal associated with the initial data, given by

$$\hat{D}(0) \triangleq \frac{1}{n_p}\sum_{n=-n_p}^{-1} D(n)\,.$$

## B. Design of the Least-Mean-Square Filter

Suppose that estimates of the parameters $A_k$, $B_k$, and $\sigma_{N,k}^2$ are available and are to be used in designing a linear FIR filter with $L$ coefficients that are subject to minimizing the mean-squared error. More precisely, let $\mathbf{W}(k) = [w(k)_1 \ldots w(k)_L]$ be a vector of $L$ coefficients representing the FIR filter. A linear estimate of $X(n)$ can be obtained as

$$(7)\ \hat{X}(n) = \sum_{i=n-L+1}^{n} w(k)_i Y(i) + \beta\,,$$

where β is a term making Eq. (7) an unbiased estimator. The filter parameters $\mathbf{W}(k)$ and β are chosen to minimize the mean-squared error defined by

$$\mathrm{E}\left[\left(\hat{X}(n) - X(n)\right)^2\right].$$

This LMS linear filter (or discrete-time Wiener filter) can be obtained by solution of the Wiener–Hopf equations associated with the minimization,[13] and the optimal filter coefficients are given by

$$(8)\mathbf{W}(k) = \mathbf{C}_{YY}(k)^{-1}\mathbf{C}_{XY}(k),$$

$$(9)\ \beta = \mu_X - (A_k\mu_X + B_k)\sum_{i=1}^{L} w(k)_i,$$

where $\mathbf{C}_{YY}(k)$ is the data covariance matrix, $\mathbf{C}_{XY}(k)$ is the cross covariance of the signal and the data, and $\mu_X$ is the mean signal and is given by $0.5(x_{max} + x_{min})$. For the model considered in Eq. (1) the above covariances are

$$(\mathbf{10})\ \mathbf{C}_{XY}(k) = \mathbf{C}_{XX}(k)A_k,$$

$$(\mathbf{11})\ \mathbf{C}_{YY}(k) = A_k^2\mathbf{C}_{XX}(k) + \sigma_{N,k}^2\mathbf{I},$$

where $\mathbf{I}$ is the $L \times L$ identity matrix and $\mathbf{C}_{XX}(k)$ is the covariance matrix of the vector $[X(n-L+1), \ldots, X(n)]'$.

In the special case when $L = 1$, the LMS filter simplifies to

$$\mathbf{W}(k) = \frac{A_k\sigma_X^2}{A_k^2\sigma_X^2 + \sigma_{N,k}^2}$$

$$\beta = \mu_X - w(k)(A_k\mu_X + B_k),$$

where

$$\sigma_X^2 = \frac{1}{12}(x_{max} - x_{min})^2$$

is the variance of a uniformly distributed random variable[14] representing the irradiance.

## C. Updating the Model Parameters

We now proceed to use the data $Y(n)$ in the range $kn_b - n_p \le n \le kn_b - 1$ in estimating the updated parameters $A_k$, $B_k$, and $\sigma_{N,k}^2$ of the $k$th block. (Recall that these updated parameters will be used in the LMS filter used to process the $k$th block of data.) The updated noise variance $\sigma_{N,k}^2$ can be computed by use of the same difference technique used in the initial parameter estimation discussed in Subsection 3.A. In particular,

$$(12)\ \sigma_{N,k}^2 \approx \frac{1}{2}\frac{1}{n_p}\sum_{n=kn_b-n_p}^{kn_b-1}\left[D(n) - \hat{D}(k)\right]^2,$$

where $\hat{D}(k)$ is the sample mean of the difference signal, given by

$$(13)\ \hat{D}(k) \triangleq \frac{1}{n_p}\sum_{n=kn_b-n_p}^{kn_b-1} D(n).$$

The parameters $A_k$ and $B_k$ are generated by means of matching the sample mean and the sample variance of $Y(n)$ with the ensemble mean and the ensemble variance of $Y_n$. More precisely, the sample mean and the sample variance of the data defined by

$$(14)\ \hat{y}(k) \triangleq \frac{1}{n_p}\sum_{n=kn_b-n_p}^{kn_b-1} Y(n),$$

$$(15)\ \hat{\sigma}_Y^2(k) \triangleq \frac{1}{n_p}\sum_{n=kn_b-n_p}^{kn_b-1}\left(Y(i) - \hat{y}(k)\right)^2,$$

respectively, are equated to the ensemble mean and the ensemble variance of $Y(n)$, which are computed by use of expression (1). In particular, if we let $\mu_X(k)$ and $\sigma_X^2(k)$ denote the mean and the variance, respectively, of the signal for the frames indexed by $kn_b - n_p \le n \le kn_b - 1$, we obtain

$$(16)\ \hat{y}(k) \approx A_k\mu_X(k) + B_k,$$

$$(17)\ \sigma_Y^2(k) \approx A_k^2\sigma_X^2(k) + \sigma_{N,k}^2.$$

Estimates of $\mu_X(k)$ and $\sigma_X^2(k)$, denoted respectively by $\mu\hat{X}(k)$ and $\sigma\hat{X}2(k)$, can be obtained if we exploit the assumption that the irradiance at each detector is a uniformly distributed random variable in a range whose upper and lower limits are obtained as follows: Recall that $\hat{X}(n)$, in the range $kn_b - n_p \le n \le kn_b - 1$, represents the estimate of $X(n)$ obtained by use of the LMS filter of the $(k-1)$th block. If we substitute the maximum and the minimum of $\hat{X}(n)$ over the prescribed range [denoted, respectively, by $x_{min}(k)$ and $x_{max}(k)$] in the formulas[14] for the mean and the variance of the uniformly distribution random variable $X(n)$, we obtain

$$(18)\ \hat{\mu}_X(k) = [x_{max}(k) + x_{min}(k)]/2,$$

$$(19)\ \hat{\sigma}_X^2(k) = [x_{max}(k) - x_{min}(k)]^2/12.$$

Now by substituting Eqs. (14) and (15) into expressions (16) and (17), respectively, and by using the estimates in Eqs. (18) and (19), we can compute the updated parameters $A_k$ and $B_k$ as the solution to a system of two linear equation with two unknowns.

## 4. Applications and Discussion

The proposed algorithm has been applied to two sets of real data from a 128 × 128 pixel InSb Amber Model AE-4128 infrared FPA camera operating in the wavelength range of approximately 3–5 μm. Terrestrial scenes are taken at two times during the day. There is a 3.5-h time lapse between the two sets of data. Two sets of parameter-estimation data are generated: A sequence of 3000 frames from the first data set is used for the initial parameter estimation, and another sequence of 3000 frames from the second data set is used to update the parameters. The parameter $n_p$, introduced in Section 3, is therefore 3000, and the block-length parameter $n_b$ is approximately $23 \times 10^6$ (corresponding to a real-time duration of 3.5 h). In capturing both sets of data the camera was moved manually by the operator.

Figure 2 shows a single frame of the uncorrected image from the first data set, and Fig. 3 shows a single frame from the second data set. In all of the examples described below, we took the length of the LMS filter as $L = 1$ and assumed that the irradiance from distinct frames was uncorrelated. This assumption simplified the design of the LMS filter and also generated good results. Note that increasing the number of coefficients $L$ will result in better blocking of temporal noise because it amounts to the temporal weighted averaging of the frames. However, the improved temporal-noise performance is accompanied by a reduction in the temporal resolution.

For purposes of comparison a black-body radiator is used under laboratory conditions to generate six sets of flat-field images in the linear range of the detectors. These data are used to estimate the gain, the offset, and the noise variance associated with each detector. These parameters are computed by the fitting of the flat-field data to the mean, the variance, and the third central moment of $Y(n)$ obtained by use of the model equations (1). These parameters are then used to design a LMS filter to compensate for the spatial noise.

As a quantitative measure of performance, we use the performance parameter ρ, which measures the roughness in an image. More precisely, for any digital image $f$, we define

$$(20)\ \rho(f) \triangleq \frac{\|h_1 * f\|_1 + \|h_2 * f\|_1}{\|f\|_1},$$

where $h_1$ is a horizontal mask [1, -1], $h_2 = h_1^T$ is a vertical mask, the asterisk denotes discrete convolution, and, for any image $f$, $\|f\|_1$ is its $L_1$ norm. (The $L_1$ norm is simply the sum of the magnitudes of all pixels.) The two terms in the numerator of Eq. (20) measure the pixel-to-pixel roughness in the horizontal and the vertical directions, respectively. Normalization by $\|f\|_1$ in Eq. (20) makes ρ invariant under scaling. Clearly, ρ is zero for a constant image, and it increases with the pixel-to-pixel variation in the image.

### A. Applying the Algorithm to an Initial Set of Data

The initial parameter estimation (as described in Subsection 3.A) of the gain $A_0$ and the offset $B_0$ is performed with 300 frames uniformly sampled from the initial 3000 frames of the first data set. The reduction in sample size is carried out to reduce computation, and it does not result in a noticeable

change in the performance. The noise parameter is computed by the application of the difference-of-frames method described in Subsection 3.A to all the 3000 frames in the first data set. The initial estimation of the noise variance, the gain, and the offset took approximately 25 min on a SUN-SPARC 120 workstation with matlab. The estimated gain is approximately 6%–10% greater than the gain computed by use of the black-body-radiation data. The offset varied approximately 16% from that computed by use of the black-body-radiation data. The standard deviation associated with data set 1 can be up to an order of magnitude higher than the one computed with the black-body radiation. This difference is expected because scene data were captured under outdoor conditions. The standard deviation of the noise, computed by use of black-body radiation, is found to be approximately 0.1% of the detector response.

Figure 4 shows the corrected version of the image in Fig. 2 when the above-described initial parameters are used in the design of the filter, as discussed in Subsection 3.B. The performance parameter ρ associated with the images in Figs. 2 and 4 are shown in Table 1 and indicate a reduction of approximately 25% in ρ after the correction. We found that, when the above initial gain and offset are updated by use of the same sample of data set 1 (with the technique described in Subsection 3.C), a significant improvement in the results is achieved. To generate these updates, we compute the range of irradiance for each detector by taking the maximum and the minimum of the initially corrected images in the 300 frames from data set 1. These statistics are then used to calculate the ensemble mean and the ensemble variance from Eqs. (18) and (19), which are subsequently used in obtaining the new gain and offset. The updated gain and offset are within approximately 21% of their initial values.

Figure 5 shows the corrected version of the image in Fig. 2 that was obtained by use of the updated LMS filter. It is clear that the updating of the gain and the offset results in a significant improvement in the performance. In fact, the performance parameter associated with Fig. 5 is only 5% greater than that associated with the image obtained by use of the calibration method (as shown in Fig. 6), as can be seen from Table 1. The performance parameter associated with Fig. 5 is approximately 36% less than that associated uncorrected image.

## B. Updating the Algorithm

Next we apply the algorithm to the second data set. The first step is to generate the updated gain, offset, and noise variance, denoted by $A_1$, $B_1$, and $\sigma_{N,1}^2$, respectively. Because the updated parameters associated with the first data set yielded improved results, we use them as a point of departure for generating the updated parameters $A_1$, $B_1$, and $\sigma_{N,1}^2$. The parameters $A_1$ and $B_1$ are generated by use of the theory presented in Subsection 3.A, and the updated noise variance $\sigma_{N,1}^2$ is generated by use of the difference-of-frames technique applied to all 3000 frames of data set 2. After these parameters are updated the updated LMS filter is constructed and used to perform NUC. For computational convenience, once again, we use a sample of only 300 frames from data set 2 to update the gain and the offset.

Figure 7 shows the corrected version of the image in Fig. 3 that was obtained by use of the updated LMS filter. The correction achieved compares well with the correction obtained by use of calibration, as shown in Fig. 8. In fact, both cases result in approximately the same performance parameter ρ, as can be seen from Table 2. The reduction in ρ is approximately 56%, which is greater than the reduction in ρ associated with data set 1 (36%).

To emphasize the role of updating the gain, the offset, and the noise variance, we attempted to perform NUC on data set 2 by using the LMS filter designed for data set 1, and the corrected image is shown in Fig. 9. By comparing Figs. 9 and 7 and by observing the parameter ρ for each image (see Table 2), we can clearly see that updating the parameters significantly improves the performance.

### C. Further Comments

The key requirement for obtaining accurate initial estimates of the gain and the offset is that the range of irradiance (that each detector is exposed to) in the initial frames must be the same for all detectors. This requirement can easily be met, for instance, if the camera is exposed to a scene with a wide range of irradiance levels and is moved as the frames are acquired, so that all detectors are exposed to approximately the same range of irradiance. The above constant-range requirement resembles the constant-statistic assumption required by other scene-based algorithms.[11],[9],[3] However, the requirement that all detectors be exposed to the same range of irradiance (i.e., all detectors are exposed to the same minimum and maximum irradiance levels) is less restrictive than the traditional constant-statistic assumption, which requires that the mean and the variance of the irradiance be common to all detectors. For example, if the detectors in the center of the array are exposed to a warm object most of the time and the detectors on the perimeter of the array are exposed to that object only a fraction of the time, then, clearly, both groups of detectors are exposed to the same range. Nonetheless, the sample mean and the sample variance of the irradiance at the two detector groups can be significantly different because of the difference in the amounts of time each detector is exposed to the warm object.

In addition to the constant-range requirement, it is also desirable that the range of irradiance in the initial data set be comparable with the actual range of irradiance required for linear operation of the detectors. Our results indicate, however, that this requirement is not as important as the constant-range requirement. In our examples both of the data sets adequately satisfied both of the foregoing requirements. In fact, the algorithm was also tested with 300 frames of another set of initial data collected in the early morning when the irradiance level is low, and the quality of correction was found to be comparable with that of the previous cases of data sets 1 and 2.

An advantage of the reported algorithm over other existing scene-based NUC algorithms[10],[9],[3] is that the constant-range assumption is required here *only* in the initial parameter estimation of the gain and offset. Subsequent updates do not require the constant-range assumption. In addition, our algorithm has the added feature of updating the noise variance, which has not been included in most of the previous algorithms.

## 5. Conclusion

We have developed a statistical technique for estimating the gain, the offset, and the temporal-noise variance of each detector in a FPA by using only scene data. The estimated parameters are used in designing a linear LMS FIR filter that compensates for the spatial nonuniformity in the array gain, the offset, and the temporal-noise variance. The initial set of data used to start the algorithm is assumed to be spatially well distributed so that all detectors in the array are exposed to approximately the same minimum and maximum irradiance. The algorithm is subsequently updated by use of new data so that the estimated values of the gain, the offset, and the noise variance of each detector are current.

The algorithm was tested with terrestrial scenes captured by an Amber infrared FPA camera. The achieved NUC was found to be comparable with the correction obtained by use of a multiple-temperature calibration technique. The examples considered showed that the algorithm is robust in the sense that, even if the initial data lack a large dynamic range, the performance of the correction is quite good. Furthermore, the updating aspect of the algorithm allows the correction filter to adapt to the temporal changes in the characteristics of the individual detectors. These temporal changes include the well-known drift in the offset that traditionally has been compensated for by means of performing frequent calibrations. Although no temporal correlation in the irradiance was considered in the examples, the algorithm can readily utilize such added information to improve performance in cases in which the initial data are extremely poor. The use of such correlation information in the algorithm is akin to high-pass filtering, which is often employed in existing scene-based NUC algorithms.

The reported algorithm has the feature that, although correction is executed on a frame-by-frame basis, the updating of the parameters of the correction filter is carried out sparingly, which reduces the computational complexity. The average number of operations per frame per pixel is approximately 10. Such a low complexity level may lead to the real-time implementation of the algorithm.

The authors thank Carl White, Jim Glidewell, Ken Barnard, and Tony Absi, at the U.S. Air Force Research Laboratory, Wright-Patterson Air Force Base, for their support of this project. This research was funded by the National Science Foundation (Career Program MIP-9733308) and the U.S. AFRL, Wright-Patterson Air Force Base.

**Figures and Tables**

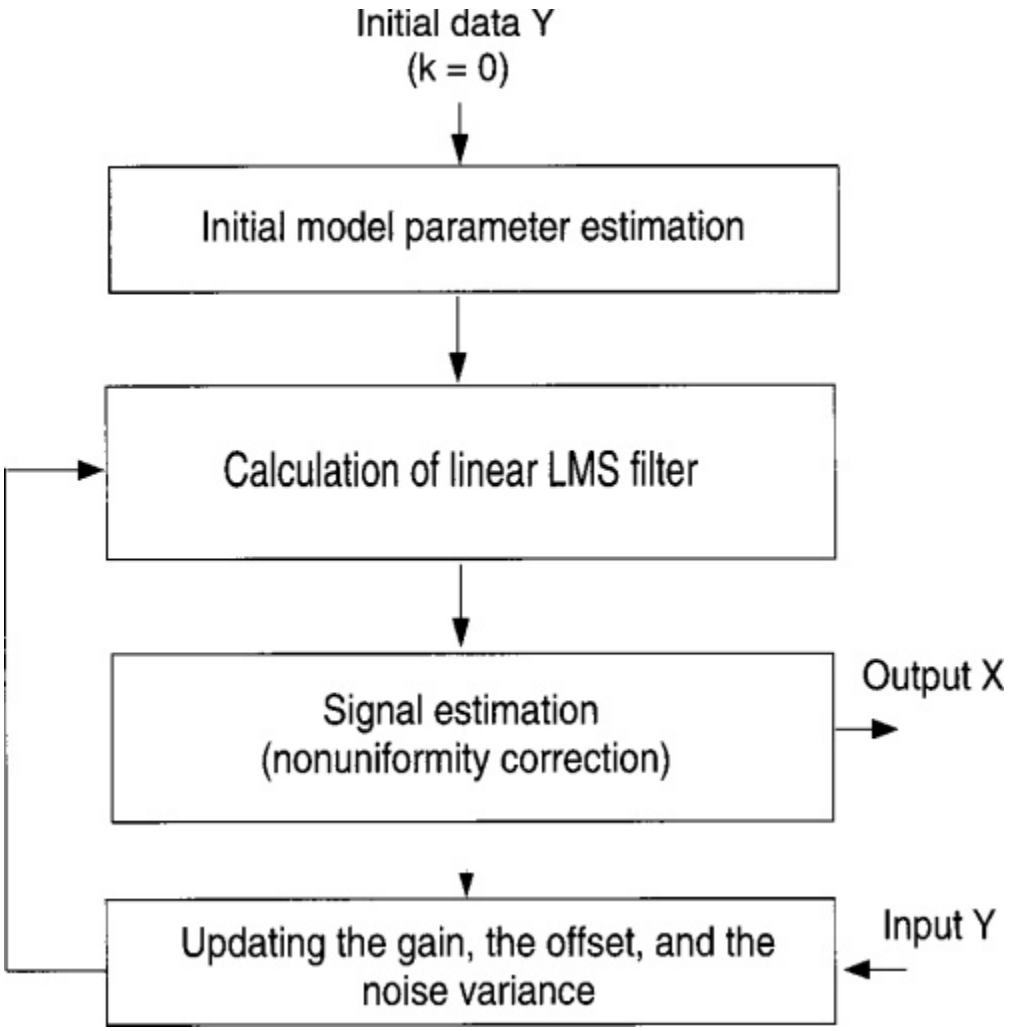


**Fig. 1** Block diagram of the statistical NUC algorithm.

**Fig. 2** Single frame from the uncorrected first data set.

**Fig. 3** Single frame from the uncorrected second data set.

**Fig. 4** Frame from Fig. 2 but with NUC by use of the initial estimates of the gain, the offset, and the noise variance.

**Fig. 5** Corrected version of the image of Fig. 2 obtained by use of the updated gain and offset. Note the improvement, which is due to recursion, in the correction compared with that of the image of Fig. 4.

**Fig. 6** Corrected version of the frame of Fig. 2 obtained by use of a multiple-point calibration method.

**Fig. 7** Corrected version of the scene from Fig. 3 obtained by use of the updated gain and offset.

**Fig. 8** Corrected version of the frame of Fig. 3 obtained by use of a multiple-point calibration method.

**Fig. 9** Corrected version of the frame of Fig. 3 obtained by use of the new algorithm but with use of the gain and the offset that correspond to data set 1. The advantage of updating the gain and the offset is evident compared with the image of Fig. 7.

| | | | Corrected Images | |
|---|---|---|---|---|
| | | | | |
| Performance Parameter | Uncorrected Image (Fig. 2) | Without Updating (Fig. 4) | With Updating (Fig. 5) | Calibration Correction (Fig. 6) |
| p | $3.4 \times 10^3$ | $2.6 \times 10^3$ | $2.2 \times 10^3$ | $2.1 \times 10^3$ |

**Table 1.** Performance Parameter ρ for Data Set 1

| | | | Corrected Images | |
|---|---|---|---|---|
| | | | | |
| Performance Parameter | Uncorrected Image (Fig. 3) | With Updating (Fig. 7) | Calibration Correction (Fig. 8) | Correction by Set 1 Filter (Fig. 9) |
| p | $4.9 \times 10^3$ | $2.2 \times 10^3$ | $2.2 \times 10^3$ | $2.9 \times 10^3$ |

**Table 2.** Performance Parameter ρ for Data Set 2

## References


**1.** A. F. Milton, F. R. Barone, and M. R. Kruer, "Influence of nonuniformity on infrared focal plane array performance," Opt. Eng. **24**, 855–862 (1985). [CrossRef]

**2.** G. C. Holst, *CCD Arrays, Cameras, and Displays*, Vol. PM57 of SPIE Monographs and Handbook Series (SPIE, Bellingham, Wash., 1996).

**3.** D. A. Scribner, K. A. Sarkay, J. T. Caulfield, M. R. Kruer, G. Katz, and C. J. Gridley, "Nonuniformity correction for staring focal plane arrays using scene-based techniques," in *Infrared Detectors and Focal Plane Arrays*, E. Dereniak and R. E. Sampson, eds., Proc. SPIE 1308, 224–233 (1990).

**4.** D. A. Scribner, M. R. Kruer, and J. C. Gridley, "Physical limitations to nonuniformity correction in focal plane arrays," in *Focal Plane Arrays: Technology and Applications*, J. P. Chatard, ed., Proc. SPIE 865, 185–201 (1988). [CrossRef]

**5.** D. L. Perry and E. L. Dereniak, "Linear theory of nonuniformity correction in infrared staring sensors," Opt. Eng. **32**, 1853–1859 (1993). [CrossRef]

**6.** M. Schulz and L. Caldwell, "Nonuniformity correction and correctability of infrared focal plane arrays," Infrared Phys. Technol. **36**, 763–777 (1995). [CrossRef]

**7.** D. A. Scribner, K. A. Sarkady, M. R. Kruer, J. T. Calufield, J. D. Hunt, M. Colbert, and M. Descour, "Adaptive retina-like preprocessing for imaging detector arrays," in *Proceedings of the IEEE International Conference on Neural Networks* (Institute of Electrical and Electronic Engineers, New York, 1993), pp. 1955–1960. [CrossRef]

**8.** D. Scribner, K. Sarkady, M. Kruer, J. Calufield, J. Hunt, M. Colbert, and M. Descour, "Adaptive nonuniformity correction for IR focal plane arrays using neural networks," in *Infrared Sensors: Detectors, Electronics, and Signal Processing*, T. S. Jayadev, ed., Proc. SPIE 1541, 100–109 (1991).

**9.** P. M. Narendra and N. A. Foss, "Shutterless fixed pattern noise correction for infrared imaging arrays," in *Technical Issues in Focal Plane Development*, W. S. Chan and E. Krikorian, eds., Proc. SPIE 282, 44–51 (1981). [CrossRef]

**10.** J. G. Harris, "Continuous-time calibration of VLSI sensors for gain and offset variations," in *Smart Focal Plane Arrays and Focal Plane Array Testing*, M. Wigdor and M. A. Massie, eds., Proc. SPIE 2474, 23–33 (1995). [CrossRef]

**11.** J. G. Harris and Y.-M. Chiang, "Nonuniformity correction using constant average statistics constraint: analog and digital implementations," in *Infrared Technology and Applications XXIII*, B. F. Anderson and M. Strojnik, eds., Proc. SPIE 3061, 895–905 (1997). [CrossRef]

**12.** S. Cain, E. Armstrong, and B. Yasuda, "Joint estimation of image, shifts, and nonuniformities from IR images," in *Proceedings of the 1997 Meeting of the Infrared Information Symposium (IRIS) Specialty Group on Passive Sensors* (Infrared Information Analysis Center, ERIM International, Ann Arbor, Mich., 1997).

**13.** H. V. Poor, *Introduction to Signal Detection and Estimation* (Springer-Verlag, New York, 1988). [CrossRef]

**14.** H. Stark and J. W. Woods, *Probability, Random Processes, and Estimation Theory for Engineers* (Prentice-Hall, Englewood Cliffs, N.J., 1994).